ELSEVIER

Seminars in
ULTRASOUND
CT *and* MRI

MRI for Traumatic Knee Injury: A Review

Edwin H.G. Oei, MD, MSc,[*,†,‡] Abida Z. Ginai, MD, PhD,[†] and M.G. Myriam Hunink, MD, PhD[*,†,‡]

Magnetic resonance imaging (MRI) is a well-established technique for detecting internal derangements of the knee joint with high diagnostic accuracy. It is an effective tool to select patients for targeted therapeutic arthroscopy. In this article, indications for knee MRI and most commonly used MRI techniques are outlined, followed by an overview of the most frequently encountered traumatic knee derangements in daily practice and their appearance and grading system on MRI. Lesions discussed include fractures, osteochondral lesions, bone bruise, cruciate and collateral ligament lesions, and meniscal tears. Finally, common pitfalls and recent developments in knee MRI are addressed.
Semin Ultrasound CT MRI 28:141-157

Magnetic resonance imaging (MRI) is a well-accepted imaging modality in the diagnostic workup of patients with knee complaints and has largely replaced diagnostic arthroscopy for this purpose.[1-4] Whereas conventional radiographs may only reveal large osseous lesions, MRI is capable of depicting soft-tissue abnormalities, such as meniscal lesions, cruciate ligament and collateral ligament lesions, tendinous lesions, and loose bodies, which may lead to targeted therapeutic arthroscopy. In addition, subtle osseous abnormalities such as radiographically occult fractures, bone marrow edema, and osteochondral lesions can be diagnosed with MRI. Previous studies have demonstrated a high diagnostic accuracy of knee MRI as compared to arthroscopy, in particular with regard to meniscal tears and cruciate ligament ruptures.[5-7] This article starts with a brief discussion on the indications for knee MRI in the setting of trauma. The most commonly used MRI examination techniques are outlined next, followed by an overview of the most frequently encountered traumatic knee abnormalities in daily practice and their MRI characteristics. Finally, several common pitfalls and recent advances in knee MRI are discussed.

*Program for the Assessment of Radiological Technology (ART Program), Rotterdam, The Netherlands.
†Department of Radiology, Erasmus MC, University Medical Center Rotterdam, Rotterdam, The Netherlands.
‡Department of Epidemiology and Biostatistics, Erasmus MC, University Medical Center Rotterdam, Rotterdam, The Netherlands.
Address reprint requests to M.G. Myriam Hunink, MD, PhD, Program for the Assessment of Radiological Technology (ART Program), and Departments of Radiology and Epidemiology and Biostatistics; Erasmus MC, University Medical Center Rotterdam, Room Ee21-40a, Dr. Molewaterplein 50, 3015 GE Rotterdam, The Netherlands. E-mail: m.hunink@erasmusmc.nl

Indications for Knee MRI

Many studies have reported on the indications for MRI of the knee joint in various clinical settings. In the context of trauma, MRI is generally considered a valuable diagnostic tool when there is a history of acute knee trauma,[8] posttraumatic limited or painful range of motion, or mechanical knee symptoms, such as catching, locking, snapping, or crepitus.[9] Previous studies have evaluated the value of MRI in the acute stage after trauma, and found that MRI has limited cost effectiveness in this setting.[10,11] MRI is therefore usually performed at a later stage if symptoms persist. Although the diagnostic performance of knee MRI is high, close correlation with the clinical history and findings on clinical examination is essential to avoid misinterpretation.[12]

MRI Examination Technique

MRI Equipment

Apart from the traditional closed whole-body MRI units, several other magnet designs exist, some of which have been designed specifically for extremity imaging (ie, dedicated extremity closed and open systems).[13] The effect of magnetic field strength, which usually varies between 0.2 and 1.5 Tesla, has been demonstrated to be of no significant influence on diagnostic performance of meniscal and cruciate ligament tears[5]; however, a high field strength system is considered necessary for high-resolution imaging of the articular cartilage. A dedicated extremity or knee coil should be used to maximize the signal-to-noise ratio.

Patient Positioning

The patient is usually imaged in the supine position with the knee nearly or fully extended and slightly rotated externally

0887-2171/07/$-see front matter
doi:10.1053/j.sult.2007.01.003

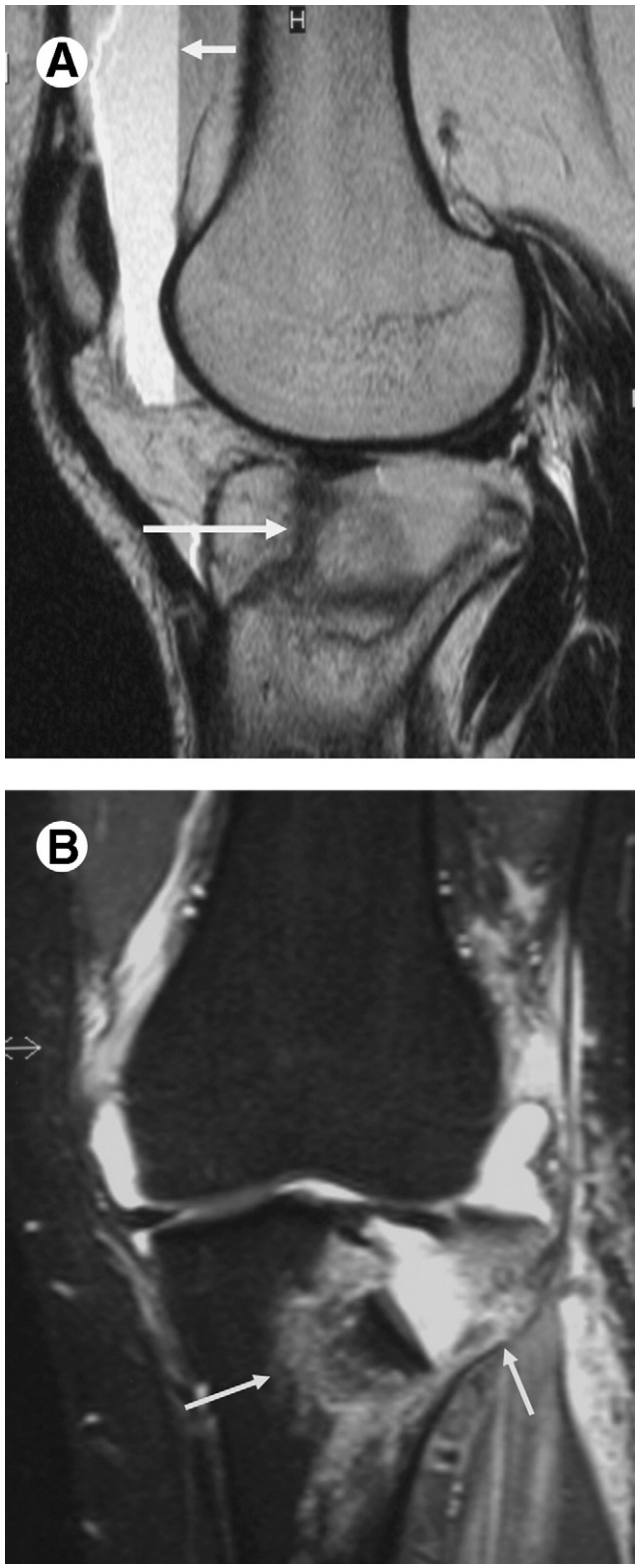

Figure 1 Fracture. (A) Sagittal T2-weighted turbo spin-echo image. Intra-articular fracture of the tibial plateau (long arrow) with an associated lipohemarthrosis in the suprapatellar recess (short arrow). (B) Coronal short tau inversion recovery image shows extensive bone marrow edema surrounding the fracture (arrows).

to align the anterior cruciate ligament parallel to the sagittal plane for better visualization.

Pulse Sequences

A wide variety of MRI pulse sequences can be performed to produce diagnostic quality images. These include spin-echo, fast (turbo) spin-echo, and gradient-echo sequences, which all have been proven suitable for knee imaging. T1- or proton density-weighted sequences are most suitable for visualizing the ligamentous anatomy. T2 or short tau inversion recovery (STIR) sequences with fat saturation are essential to demonstrate bone marrow edema. Typically, a routine scanning protocol would consist of a combination of one or more of these sequence types performed in the axial, sagittal, and coronal planes using thin sections (maximum 3 mm with an interslice gap of 0.5 to 1 mm). A field-of-view of 12 to 16 cm depending on patient size is commonly used with a high-resolution matrix of at least 140 steps in the phase-encoding direction and 256 steps in the frequency-encoding direction. Although many institutions use standardized protocols for routine scanning, individual tailoring is necessary to yield optimal diagnostic performance for specific clinical queries. For example, a thin section axial sequence should be included in the protocol if damage to the patellofemoral joint is suspected and a coronal T2-weighted sequence is necessary to demonstrate collateral ligament lesions.

Figure 2 Avulsion fracture. Coronal proton density-weighted turbo spin echo image shows an avulsion fracture of the fibular head at the insertion of the conjoint tendon of the fibular collateral ligament and biceps femoris tendon (arrow).

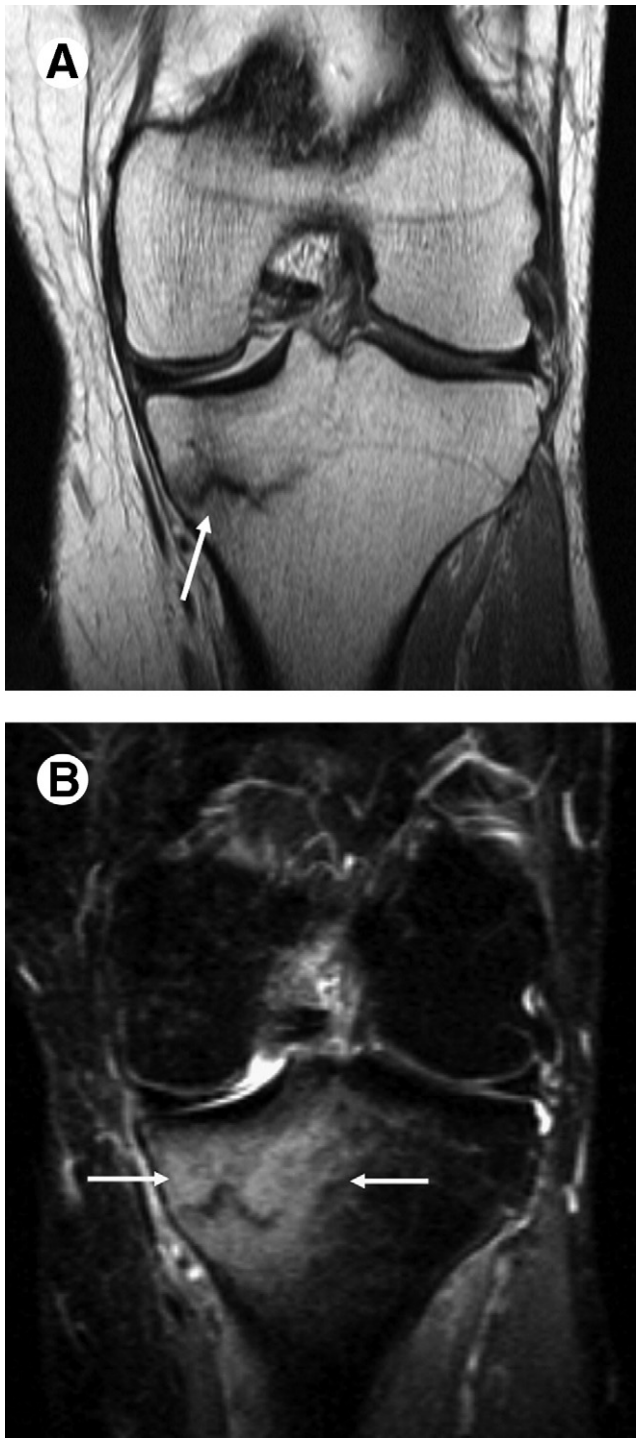

Figure 3 Stress fracture. (A) Coronal proton density-weighted turbo spin echo image. Running athlete with recurrent pain on the medial side of the knee. A stress fracture is demonstrated in the medial tibial metaphysis (arrow), which was not visible on plain radiography. (B) Coronal short tau inversion recovery image. There is extensive bone marrow edema surrounding the stress fracture (arrows).

Osseous and Chondral Lesions

Fractures and Dislocations

Occasionally, fractures may be invisible on conventional radiographs. If a fracture is strongly suspected, tomographic techniques such as computed tomography (CT) and MRI may be indicated to reveal a radiographically occult fracture. Fracture lines appear as dark signal intensity lines on all pulse sequences, and are usually surrounded by areas of bone bruise visible on fat-saturated images (Fig. 1). In case of an intra-articular fracture, fatty bone marrow will leak into the joint space, resulting in a lipohemarthrosis, which is usually visible in the suprapatellar recess (Fig. 1A). MRI may also be used to demonstrate avulsion fractures, which can be hard to diagnose on plain radiography if there is no displacement[14] (Fig. 2). Stress fractures may also be difficult to diagnose on plain radiographs, but are well visualized on MRI (Fig. 3). In the setting of a radiographically demonstrated fracture, CT with multiplanar and three-dimensional (3D) reconstructions is often performed to demonstrate the exact course of the fracture lines to guide treatment planning. MRI is, obviously, more suitable for evaluating associated soft-tissue lesions.[15,16] Likewise, MRI may be helpful in assessing the full extent of ligamentous disruptions that are invariably present after knee dislocation, as well as demonstrate additional osseous, vascular, or nervous injuries.[17] Patellar dislocations are commonly associated with rupture of the medial patellar retinaculum and this may be well visualized on axial MRI sequences.[18]

Bone Marrow Edema/Bone Bruise

Bone marrow edema is most easily identified on T2 or STIR sequences with fat suppression on which it appears as an area

Figure 4 Bone marrow edema. Coronal short tau inversion recovery image shows bone marrow edema in the medial femoral condyle (long arrow) in a patient who sustained a direct hit to the medial side of the knee. In addition, soft-tissue edema is seen superficial to the iliotibial tract (short arrow), indicating a grade 1 lesion or sprain.

of high signal intensity (Fig. 4). Bone bruise can occur as an isolated finding usually after a direct hit. More often, though, it is associated with other abnormalities such as ligamentous lesions, and frequently a typical pattern of bone bruise according to type of injury is seen.[19] For example, during the mechanism of complete anterior cruciate ligament (ACL) rupture, a transient subluxation combined with impaction between the lateral femoral condyle and the posterolateral aspect of the tibial plateau typically occurs, resulting in a characteristic pattern of bone marrow edema in these locations, which is sometimes referred to as a "kissing contusion" (Fig. 5).

Articular Cartilage Lesions

Damage to the articular cartilage may be caused by acute trauma, but more commonly is the result of chronic repetitive trauma or degenerative change. It may be difficult to distinguish between an acute and chronic chondral lesion, but analyzing the pattern of concurrent lesions such as ligament tears and bone bruise may help in the diagnosis. Osteochondritis dissecans is a local defect of the articular surface most commonly seen in adolescents and young adults. It is usually caused by repetitive trauma and MRI findings range from subchondral edematous changes to complete separation of an osteochondral fragment from the surrounding subchondral bone. Several grading systems exist, which all refer to the integrity of the articular surface and demarcation and stability of the osteochondral fragment[20] (Fig. 6). Chondromalacia is usually diagnosed in the setting of degenerative change and is therefore not discussed here.

Figure 5 Kissing contusion. Sagittal T1-weighted 3D fast field echo with spectral presaturation inversion recovery (SPIR) image. Patient with complete ACL rupture following skiing injury. Bone marrow edema is seen in the lateral femoral condyle (long arrow) and the posterolateral aspect of the tibial plateau (short arrow), a so-called kissing contusion, which typically occurs due to the trauma mechanism of a total ACL rupture.

Figure 6 Osteochondritis dissecans. Sagittal T2-weighted turbo spin echo image shows a large defect of the articular surface of the medial femoral condyle (long arrow). Since there is complete detachment of an osteochondral fragment (dislocated to the intercondylar notch, not shown), this lesion was classified as grade 4 osteochondritis dissecans. In addition, a Baker's cyst is present (short arrow), which is most often associated with internal derangements of the knee joint or degenerative osteoarthritis.

Ligamentous Injury

Cruciate Ligament Tears

Anterior Cruciate Ligament (ACL)

The ACL is an intracapsular extrasynovial structure composed of two separate bundles of fibers and is usually evaluated on T2-weighted or proton density-weighted images, where it appears as a straight low-signal intensity band running from the medial aspect of the lateral femoral condyle to the tibial plateau adjacent to the anterior tibial spine. The ACL is usually well evaluated in the sagittal plane, but images in the axial and coronal plane can be helpful in assessing the femoral and tibial attachments (Fig. 7).

Primary signs of a total ACL rupture are a complete disruption of the ACL fibers, abnormal signal intensity within the ligament and in the surrounding region, abnormal slope of the ACL, and nonvisualization of ACL fibers both in the sagittal and coronal planes (Fig. 8). Hemorrhage and edema may appear as an amorphous mass producing mass effect. Many indirect signs of ACL rupture have been described,

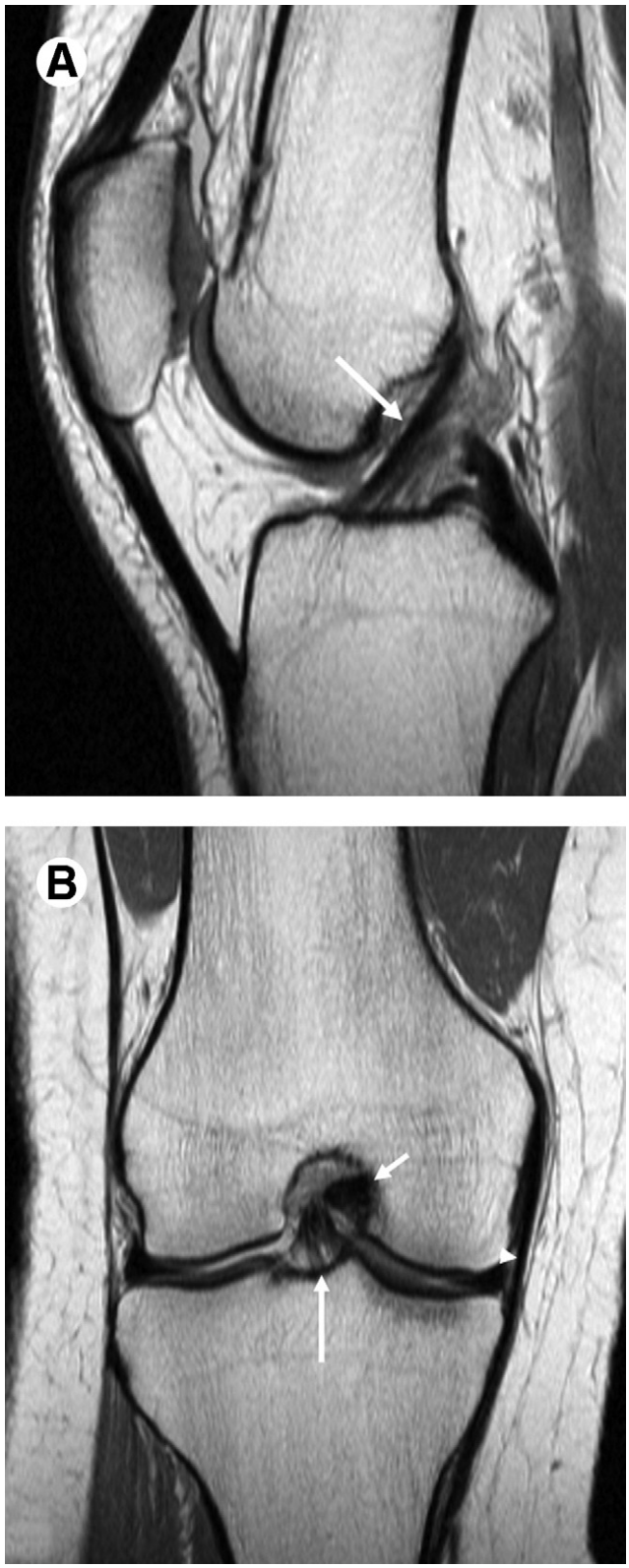

Figure 7 Normal ACL. (A) Sagittal proton density-weighted turbo spin echo image demonstrates the normal ACL as a straight low signal intensity band running from the medial aspect of the lateral femoral condyle to the tibial plateau (arrow). (B) On the coronal proton density-weighted image the insertion site of the ACL on the tibial plateau is well visualized (long arrow). In addition, the attachment of the PCL on the lateral aspect of the medial femoral condyle (short arrow) and a normal MCL (arrowhead) are seen.

such as the "anterior drawer sign," "buckled PCL sign," and the aforementioned "kissing contusion."[21-24] The anterior drawer sign refers to an abnormally anterior position of the tibial plateau relative to the femoral condyle in the extended knee, which is normally prevented by an intact ACL. Related to this is a buckled appearance of the PCL on sagittal images (the buckled PCL sign), which is caused by the abnormal alignment of femur and tibia (Fig. 9). The presence of one or more of these indirect signs increases the likelihood of, but does not rule out, an ACL rupture. Usually, however, the diagnosis of complete ACL rupture can be made using primary signs alone. In partial ACL ruptures, focal areas of high signal may be seen within the ACL, with largely intact fibers and a clinically stable knee (Fig. 10). Partial ACL ruptures are difficult to diagnose and differentiate from complete tears and clinical correlation is essential.[25]

Posterior Cruciate Ligament (PCL)

The normal PCL is visualized as a dark structure running from the lateral aspect of the medial femoral condyle to attach on the posterior tibial plateau (Figs. 7B and 11). Since it is composed of one bundle of fibers, it appears more uniformly hypointense than the ACL. The same primary signs of ACL rupture can be applied to the PCL (Fig. 12). Isolated PCL lesions are rare and PCL ruptures most commonly occur due to a direct blow on the anterior tibia with a flexed knee in the setting of a "dashboard injury."[26]

Collateral Ligament Tears

Medial Collateral Ligament (MCL)

The MCL can be divided into two layers: the superficial fibers and the deep fibers that are attached to the joint capsule and the medial meniscus. The two layers are separated by a potential space, the tibial collateral bursa, which can be filled with fluid in the setting of a MCL lesion. The MCL is best visualized on coronal images where it appears as a dark band extending from the medial femoral condyle to insert on the medial aspect of the tibia approximately 4-5 cm below the joint line (Fig. 7B). Lesions of the MCL are graded as follows: Grade 1 (sprain) lesions are defined as high signal intensity superficial to the MCL representing edema, with intact MCL fibers (Fig. 13A). In grade 2 (partial tear) lesions, fluid signal extends partially through the MCL, although some fibers remain intact (Fig. 13B). In grade 3 lesions, complete discontinuity of the MCL fibers is seen along with surrounding edema, consistent with a complete rupture (Fig. 13C). MCL injuries are usually caused by valgus stress, and are often associated with other knee derangements. The combination of an ACL tear, MCL tear, and medial meniscal tear occurs with valgus stress to the knee while the foot is fixed on the ground, and is also known as the "unhappy triad" or O'Donoghue's triad.[27]

Lateral Collateral Ligament (LCL)

The LCL complex consists of several individual components. The fibular collateral ligament (or the lateral collateral ligament proper) extends from the lateral femoral condyle and merges with the biceps femoris tendon to form the conjoint

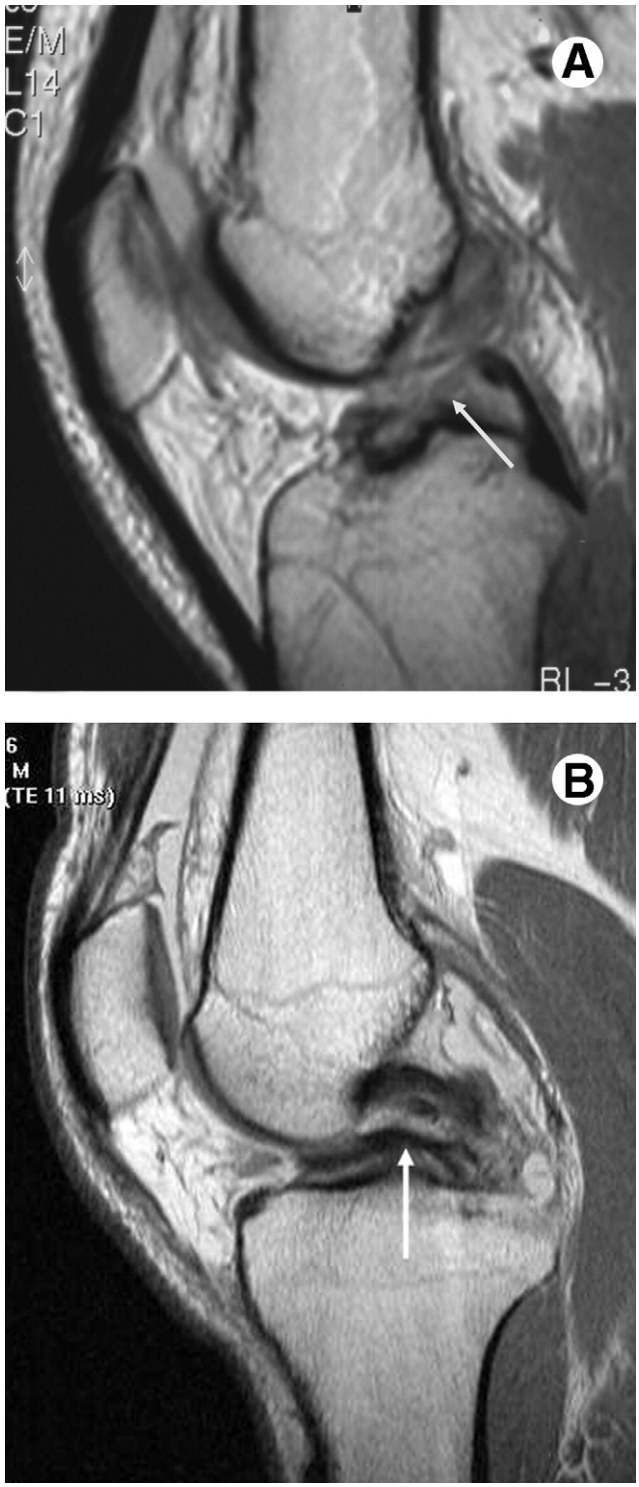

Figure 8 Complete ACL rupture. Sagittal proton density-weighted turbo spin echo images. (A) Nonvisualization of continuous ACL fibers with amorphous high signal intensity material in this area (arrow), consistent with complete ACL rupture. (B) Complete disruption of the ACL fibers with the completely torn ACL lying on the tibial plateau (arrow), resembling the "double PCL sign" that can be seen with bucket handle meniscal tears.

tendon, which inserts on the fibular head. The iliotibial tract is a continuation of the tensor fascia lata and inserts at Gerdy's tubercle on the anterolateral aspect of the tibia (Fig. 4). Like the MCL, the LCL is best visualized on coronal images. Lateral collateral ligament injuries are usually classified similarly as medial collateral ligament lesions, using the 3-point grading system as outlined above. Lesions of the LCL are most often caused by varus stress and therefore may be associated with impression fractures of the medial tibial plateau. In addition, LCL ruptures are frequently seen together with other injuries of the posterolateral corner[28] (Fig. 14).

Meniscal Pathology

The menisci serve an important role in knee function, stability and load transmission, and are composed of fibrocartilage fibers. These are oriented mostly in a circumferential manner in the peripheral one third of the meniscus and both transverse and circumferential in the central two thirds of the meniscus. Because of this difference, the periphery of the meniscus is biomechanically more important than the inner part, and consequently a torn meniscus can still facilitate load transmission as long as the periphery remains intact. The periphery of the meniscus is vascularized and appears as the "red zone" on arthroscopy. Therefore, a tear that is confined to the periphery has greater healing potential than a tear that

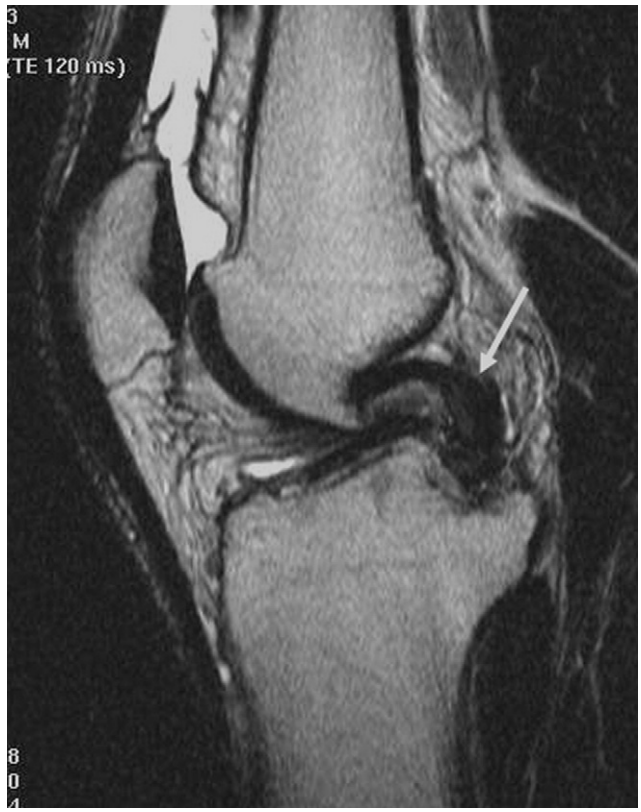

Figure 9 Buckled PCL sign. Sagittal T2-weighted turbo spin echo image. Abnormal alignment of the femur and tibia due to complete ACL rupture, resulting in a buckled appearance of the PCL, the so-called buckled PCL sign (arrow).

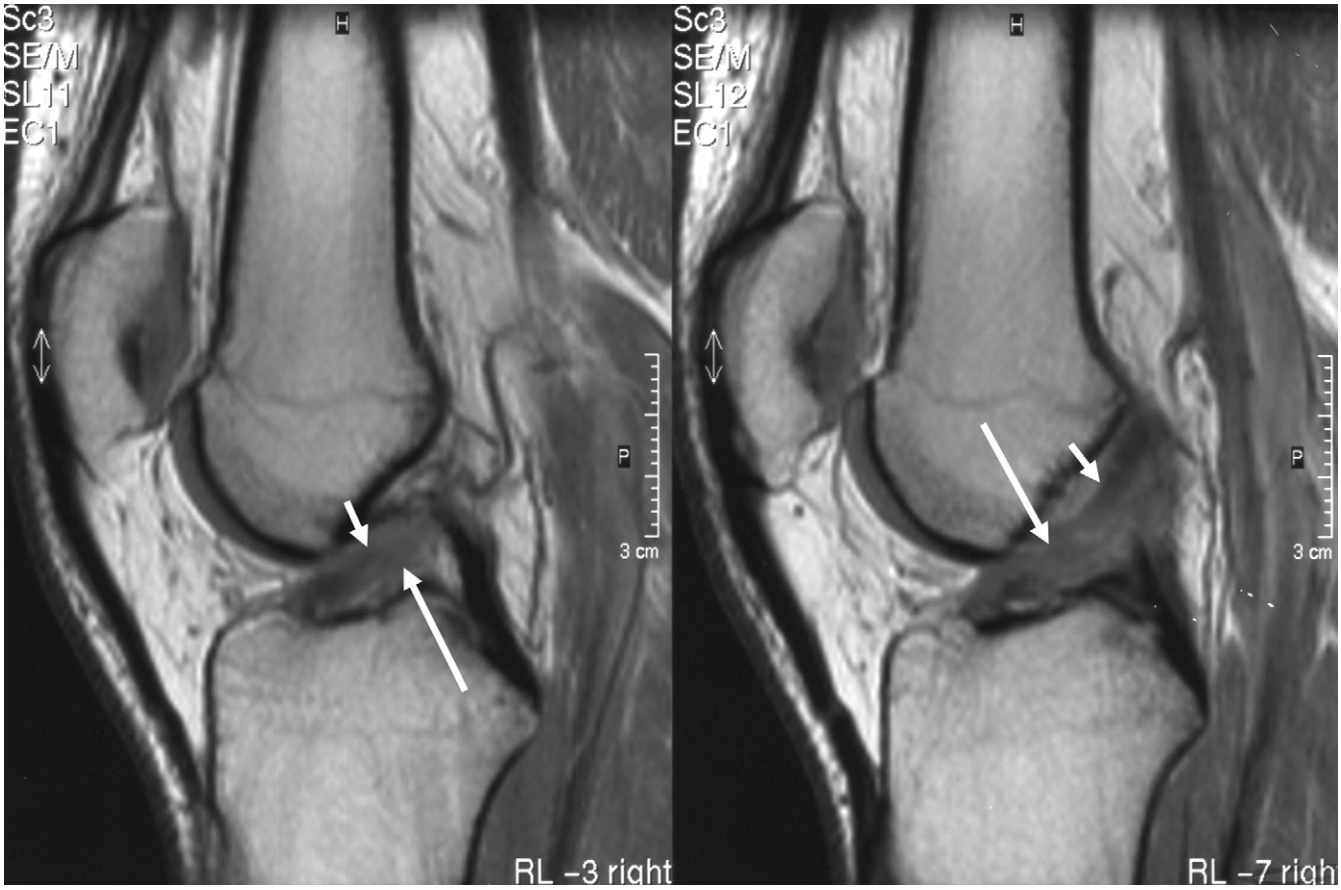

Figure 10 Partial ACL rupture. Two consecutive sagittal proton density-weighted turbo spin echo images. Focal areas of high signal intensity are seen in the course of the ACL, with partial discontinuity of the ACL fibers (long arrows). A couple of intact fibers are also noted (short arrows). Since the knee was stable on physical examination, this lesion was interpreted as a partial or subtotal ACL rupture.

also involves the avascular central portion, also known as the "white zone" arthroscopically.

Depending on the section, the normal MRI appearance of the meniscus on sagittal sections is either that of a single bow-tie shaped structure in the periphery or two triangles with facing apices representing the anterior and posterior horns more centrally (Fig. 15). The anterior and posterior horns of the lateral meniscus are approximately equal in size, whereas the posterior horn of the medial meniscus is nearly twice as large as the anterior horn.[29] The normal meniscus demonstrates low signal intensity on all pulse sequences, and should be evaluated on both sagittal and coronal images.

Meniscal Tears

Two criteria for diagnosing a meniscal tear are commonly used: (1) an intrasubstance area of intermediate or high signal intensity that unequivocally extends to the articular surface, and (2) abnormal meniscal morphology.[30,31] Intrasubstance signal is graded as follows: Grade 1 represents intrameniscal high signal intensity of irregular or globular appearance that is confined within the meniscus and does not extend to the articular surface (Fig. 16A). In grade 2 the signal is linear and does not intersect the inferior or superior articular surface (Fig. 16B). It may, however, contact the capsular margin at the posterior aspect of the meniscus. Both grade 1 and grade 2 lesions do not represent a tear, but indicate mucinous and mucoid intrasubstance degenerative change and are usually encountered after the third or fourth decade.[32] In children and adolescents, prominent vasularity may resemble grade 1 or grade 2 lesions. Grade 3 lesions represent meniscal tears and are characterized by linear high or intermediate signal intensity that extends to the superior and/or inferior articular surface (Fig. 16C). Grade 4 is sometimes added to indicate a complex tear with multiple components or fragmentation (Fig. 16D). Several types of tears with different etiology, prognosis, and treatment should be distinguished. Horizontal tears, also called degenerative tears, are considered the result of severe meniscal degeneration and most commonly affect the posterior horn of the medial meniscus. These tears are usually asymptomatic and therefore often left untreated. Radially or longitudinally oriented tears and complex tears are most often the result of trauma and usually symptomatic.[33] They have the tendency

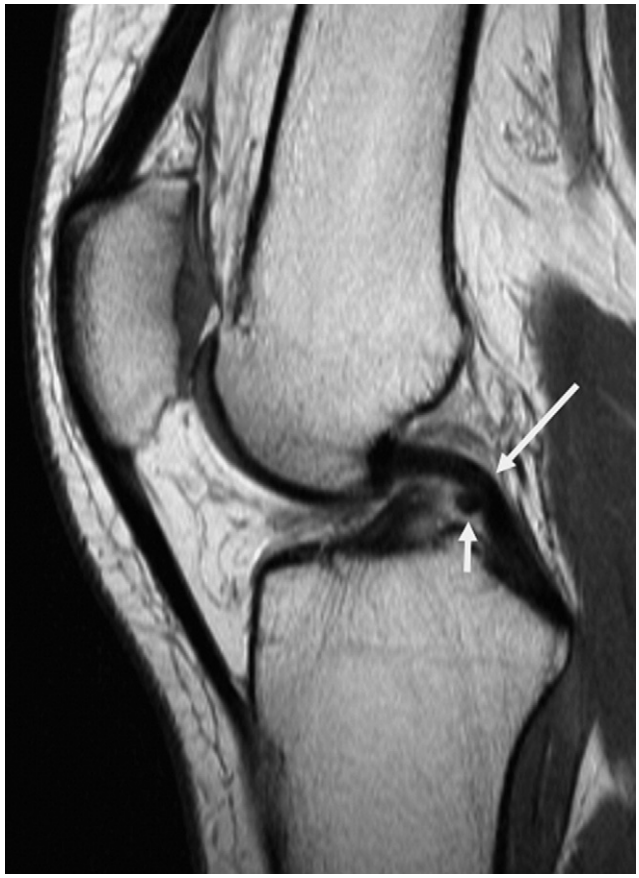

Figure 11 Normal PCL. The normal PCL is visualized as a dark band running from the lateral aspect of the medial femoral condyle to the posterior tibial plateau (long arrow) on this sagittal proton density-weighted turbo spin echo image image. Also note the presence of a meniscofemoral ligament of Humphrey (short arrow), which may mimic a loose body.

to progress in size or complexity, and fragmentation may occur, which can cause severe symptoms such as locking or snapping. Treatment, which nowadays typically consists of arthroscopic partial meniscectomy, is usually indicated in these cases.

Several secondary signs of a meniscal tear have been reported, most of which are related to the presence of a "bucket-handle tear."[34-36] This is a specific type of vertical or oblique tear in the posterior horn that extends longitudinally toward the meniscal body and anterior horn, usually with displacement of the central meniscal portion toward the intercondylar notch (Fig. 17A). The displaced fragment (the "handle") may be seen under the PCL on sagittal images, resulting in the so-called double PCL sign[37,38] (Fig. 17B). The "absent bow-tie sign" refers to the absence of the normal bow-tie-shaped appearance of the meniscal periphery in the sagittal plane, due to the displacement of the central portion in the presence of a bucket-handle tear.[39,40] The "flipped meniscus sign" refers to a meniscal fragment originating from the posterior horn or the entire posterior horn that has moved anteriorly to sit directly adjacent to or on the anterior horn of the ipsilateral meniscus, which may give the appearance of an abnormally large anterior horn[41] (Fig. 18).

Discoid Meniscus

A discoid meniscus is considered a developmental abnormality and is characterized by partial or complete covering of the central portion of the tibial plateau by meniscal tissue. Discoid menisci are far more common on the lateral side and may cause mechanical symptoms when there is extension into the intercondylar notch. They are also associated with an increased risk both of degenerative abnormalities and tears. On MRI, a discoid meniscus can be diagnosed on sagittal images through the midportion of the knee, where a continuity between the anterior and posterior horns is seen instead of the normal bow-tie and triangular appearance[42] (Fig. 19A). On coronal images, the discoid meniscus appears abnormally wide and the diagnosis can be made if it measures more than 15 mm in width[43] (Fig. 19B).

Meniscal Cyst

A meniscal cyst is a fluid-filled structure adjacent to a meniscus, which appears as an intermediate signal intensity mass on T1-weighted images and hyperintense on T2-weighted images, sometimes lobulated or septated. Meniscal cysts are strongly associated with a horizontal cleavage tear of the meniscus and often a connecting neck between the tear and the cyst can be visualized[44,45] (Fig. 20). The cysts may become fairly large, which is thought to be caused by a ball valve mechanism. They can become symptomatic usually on the medial side, since they may impress on the medial collateral ligament. Meniscal cysts tend to recur following resection or aspiration, especially if the underlying meniscal tear is left untreated.

Pitfalls

There are several pitfalls to be aware of when interpreting knee MRI, most of which are related to normal anatomical structures or normal variants that may mimic loose meniscal fragments or tears. For example, the transverse meniscal ligament may be falsely interpreted as a tear of the anterior horn of the lateral meniscus (Fig. 21). Similarly, the meniscofemoral ligaments of Humphrey (Fig. 11) and Wrisberg (Fig. 22) may mimic loose bodies or tears in the posterior horn of the lateral meniscus. The space between the periphery of the posterior horn of the lateral meniscus and popliteus tendon may resemble a rupture of the posterior horn of the lateral meniscus. Misinterpretation can be avoided by tracing the suspicious structure on sequential images. The free edge of the meniscus may occasionally demonstrate a wavy or wrinkled shape (Fig. 23). This so-called meniscal flounce most often involves the medial meniscus and is considered a normal variant or a transient physiologic distortion that may vary according to knee position.[46] The presence of a meniscal flounce does not increase the likelihood of a meniscal tear.[47,48] A potential pitfall in the interpretation of cruciate ligament tears is the ACL or PCL ganglion, which is shown as a focal globular area of fluid signal within or adjacent to the ligament (Fig. 24). Distortion of the ligament may occur due to mass effect. The presence of a focal well-defined collection

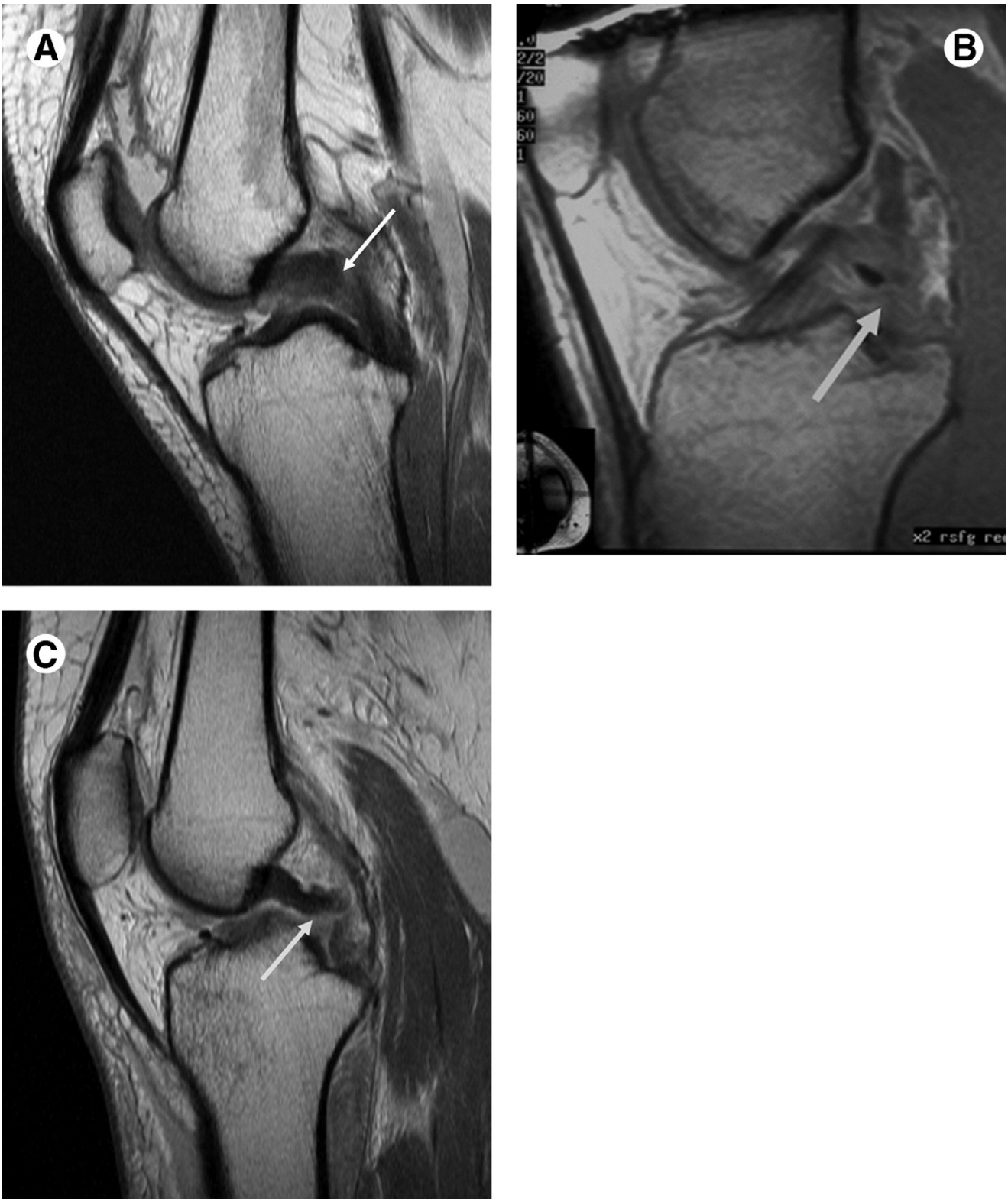

Figure 12 PCL ruptures. Sagittal proton density-weighted turbo spin echo images. (A) Thickened PCL with focal areas of high signal intensity and partial discontinuity of the PCL fibers (arrow), consistent with a partial PCL rupture. (B) Complete nonvisualization of the PCL fibers with high signal intensity in this area (arrow), indicating a PCL rupture. (C) Complete disruption of all PCL fibers indicative of a complete midsubstance tear of the PCL (arrow).

Figure 13 MCL lesions. (A) Coronal turbo inversion recovery magnitude image demonstrates edema surrounding intact MCL fibers (arrow), consistent with a grade 1 lesion. (B) Coronal T2-weighted turbo spin echo image shows a partial disruption of the MCL fibers with surrounding edema and a wavy appearance of the remaining fibers (arrow), indicating a grade 2 (partial) rupture. (C) A complete (grade 3) rupture of the MCL is visualized on this coronal short tau inversion recovery image. Complete discontinuity of the MCL fibers is seen with extensive soft-tissue edema in this region (arrow).

Figure 14 Complete LCL rupture. Coronal T2-weighted turbo spin echo image. There is complete discontinuity of the LCL and biceps femoris tendon (arrow), indicating a total rupture. Extensive soft-tissue edema is seen in this region. In addition, the patient had severe injury to the posterolateral corner, including rupture of the posterior joint capsule, as well as a total ACL rupture and partial PCL rupture.

and the absence of other signs of traumatic injury are key to the correct diagnosis.[49]

Recent Developments

Similar to those in other body areas, MRI techniques for knee imaging continue to evolve. The introduction of high-field 3.0-T MRI scanners for clinical practice has created new possibilities to image knee lesions with increased signal-to-noise ratio (SNR). This can be invested in shorter scanning time or increased spatial resolution. Recent studies have reported excellent image quality of 3.0-T knee MRI, but some of the studies also conclude that 3.0-T MRI is more prone to magnetic susceptibility artifacts and chemical shift artifacts than 1.5-T imaging.[50-53] Further research is needed to assess the advantages of 3.0-T versus 1.5-T MRI, in particular whether better image quality also improves diagnostic performance and patient management. In recent years, there has been great interest in the imaging of articular cartilage. This is mainly because of the introduction of new therapeutic options for chondral defects, such as autologous chondrocyte transplantation, where detailed preoperative evaluation and posttreatment follow-up are important.[54,55] MRI imaging of cartilage has been controversial and the reported diagnostic performance of traditional 2D fast spin echo (FSE) and 3D spoiled gradient echo (SPGR) sequences vary. Better results have been reported with novel cartilage-specific pulse sequences, such as 3D SPGR with spatial pulses (SS-SPGR)[56] and 3D steady-state free precession (SSFP) sequences.[57,58] Recent studies have shown promising results with cartilage imaging at 3.0 T,[59,60] but more research is required before these techniques can be applied in daily clinical practice.

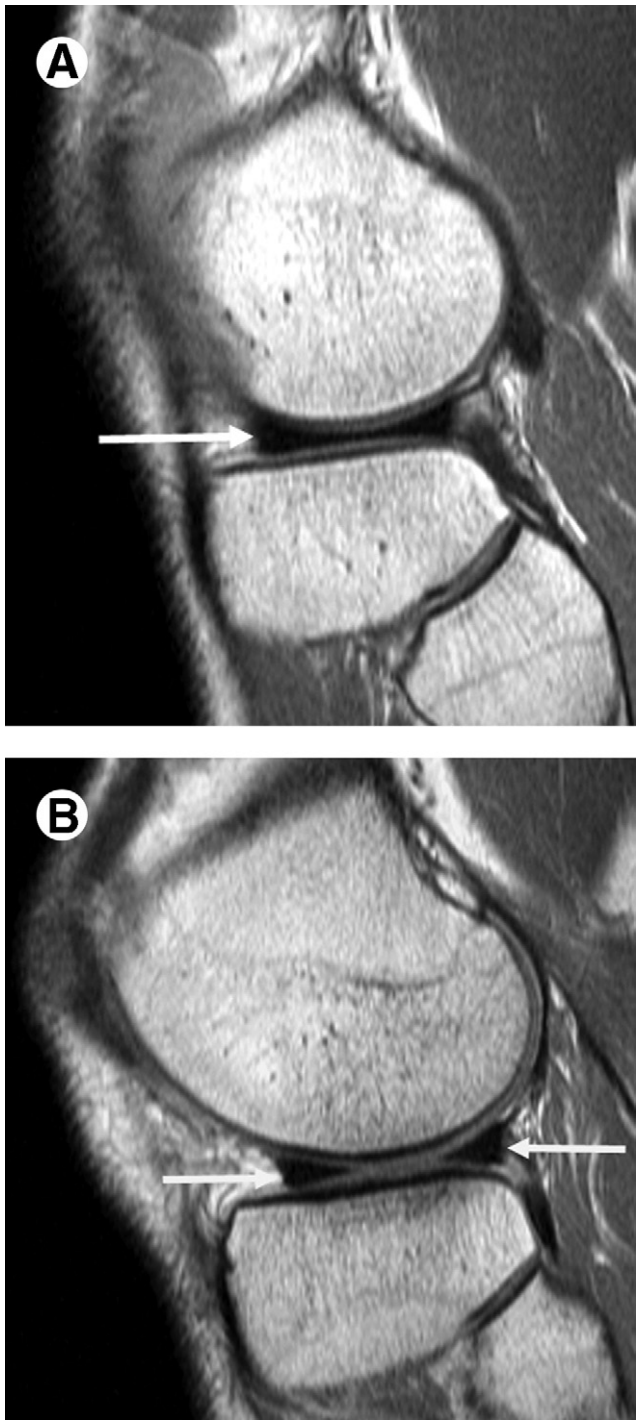

Figure 15 Normal lateral meniscus. Sagittal proton density-weighted turbo spin echo images. (A) In the peripheral part, the normal meniscus demonstrates a single bow-tie-shaped configuration (arrow). (B) More centrally, the normal meniscus is visualized as two triangles with facing apices representing the anterior and posterior horns (arrows).

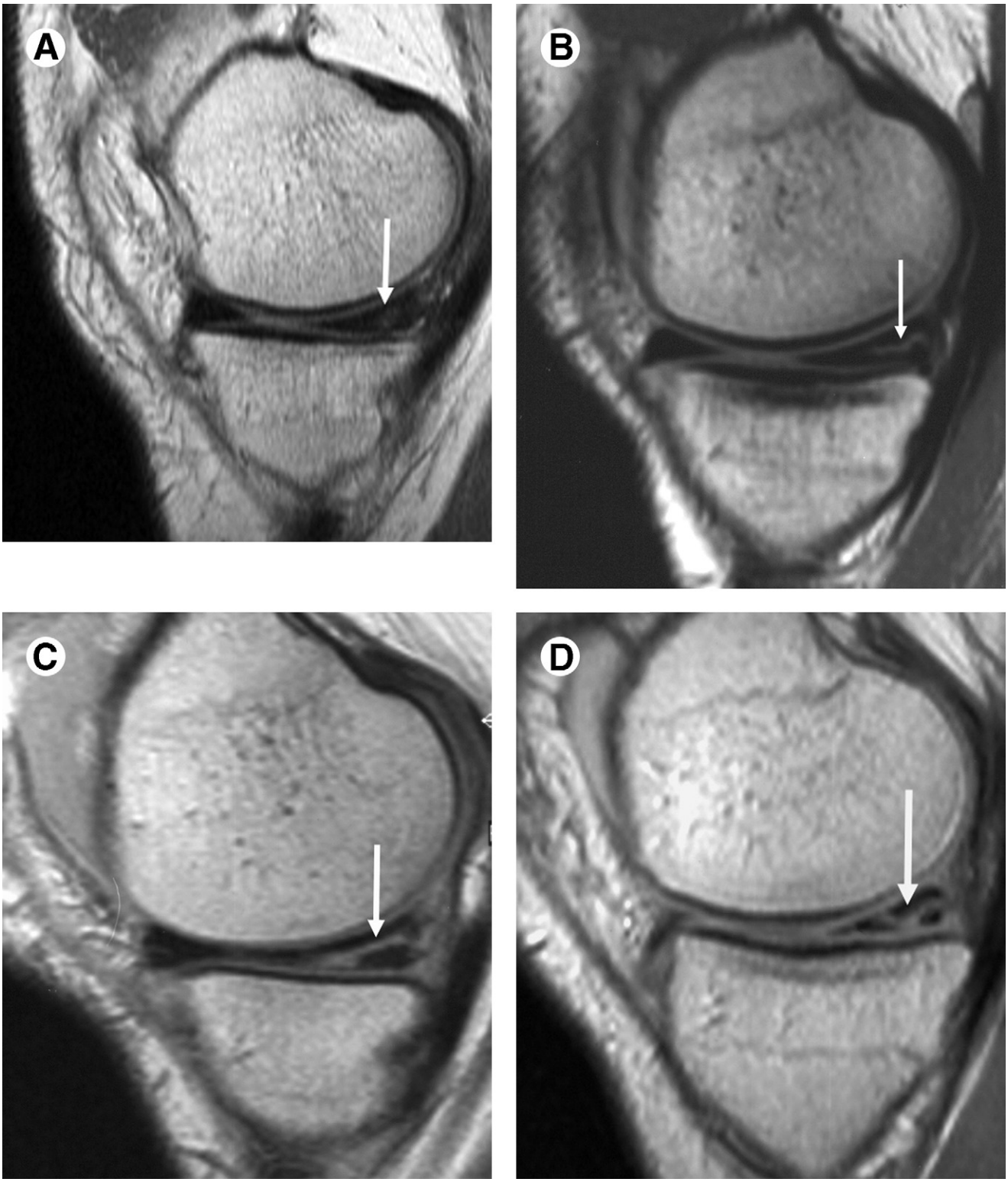

Figure 16 Grading system of meniscal lesions. Sagittal proton density-weighted turbo spin echo images of the medial meniscus. (A) Globular high intermediate signal intensity that does not extend to the articular surface (arrow) representing a grade 1 lesion (degenerative change). (B) Linear high signal that does not extend to the inferior or superior articular surface (arrow), indicating a grade 2 lesion (degenerative change). (C) Linear high signal intensity that intersects the inferior articular surface (arrow) representing a grade 3 lesion (meniscal tear). (D) Complex grade 4 tear extending to both the superior and inferior articular surfaces (arrow).

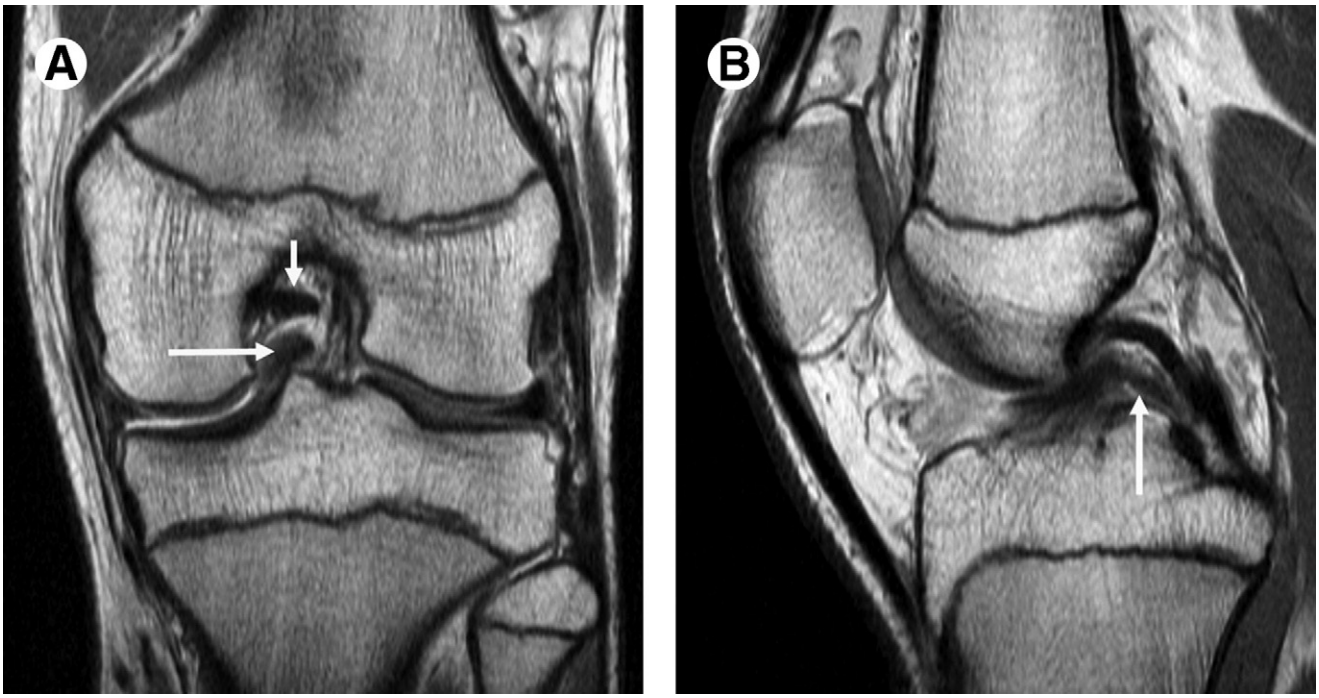

Figure 17 Bucket handle tear of the posterior horn of the medial meniscus. (A) The displaced meniscal fragment (the "handle") is visualized in the intercondylar notch (long arrow) under the PCL (short arrow) on this coronal proton density-weighted turbo spin echo image. (B) Sagittal proton density-weighted image shows the displaced fragment parallel to the PCL (arrow), the so-called double PCL sign.

Figure 18 Flipped meniscus sign. Sagittal proton density-weighted turbo spin echo images of the lateral meniscus shows a bucket handle tear of the posterior horn. A meniscal fragment has been displaced anteriorly (arrow), resulting in the appearance of an abnormally large anterior horn, the so-called flipped meniscus sign.

Summary

This review article illustrates that MRI is an effective and accurate technique in the diagnostic workup of traumatic knee abnormalities, and that it is an appropriate screening tool for therapeutic arthroscopy. The MRI interpretation and classification of the most frequently encountered traumatic knee abnormalities were discussed. One should be aware of several pitfalls in the diagnosis of meniscal tears and cruciate ligament tears. Recent advantages in knee MRI mainly focus on 3.0-T imaging and cartilage imaging, but further research in these areas is warranted.

References

1. Ruwe PA, Wright J, Randall RL, Lynch JK, Jokl P, McCarthy S: Can MR imaging effectively replace diagnostic arthroscopy? Radiology 183(2): 335-339, 1992
2. Bui-Mansfield LT, Youngberg RA, Warme W, Pitcher JD, Nguyen PL: Potential cost savings of MR imaging obtained before arthroscopy of the knee: evaluation of 50 consecutive patients. AJR Am J Roentgenol 168(4):913-918, 1997
3. Vincken PW, Ter Braak BP, Van Erkel AR, et al: Effectiveness of MR imaging in selection of patients for arthroscopy of the knee. Radiology 223(3):739-746, 2002
4. Vincken PW, Ter Braak AP, Van Erkel AR, et al: MR imaging: effectiveness and costs at triage of patients with nonacute knee symptoms. Radiology 242(1):85-93, 2007
5. Oei EH, Nikken JJ, Verstijnen AC, Ginai AZ, Myriam Hunink MG: MR imaging of the menisci and cruciate ligaments: a systematic review. Radiology 226(3):837-848, 2003

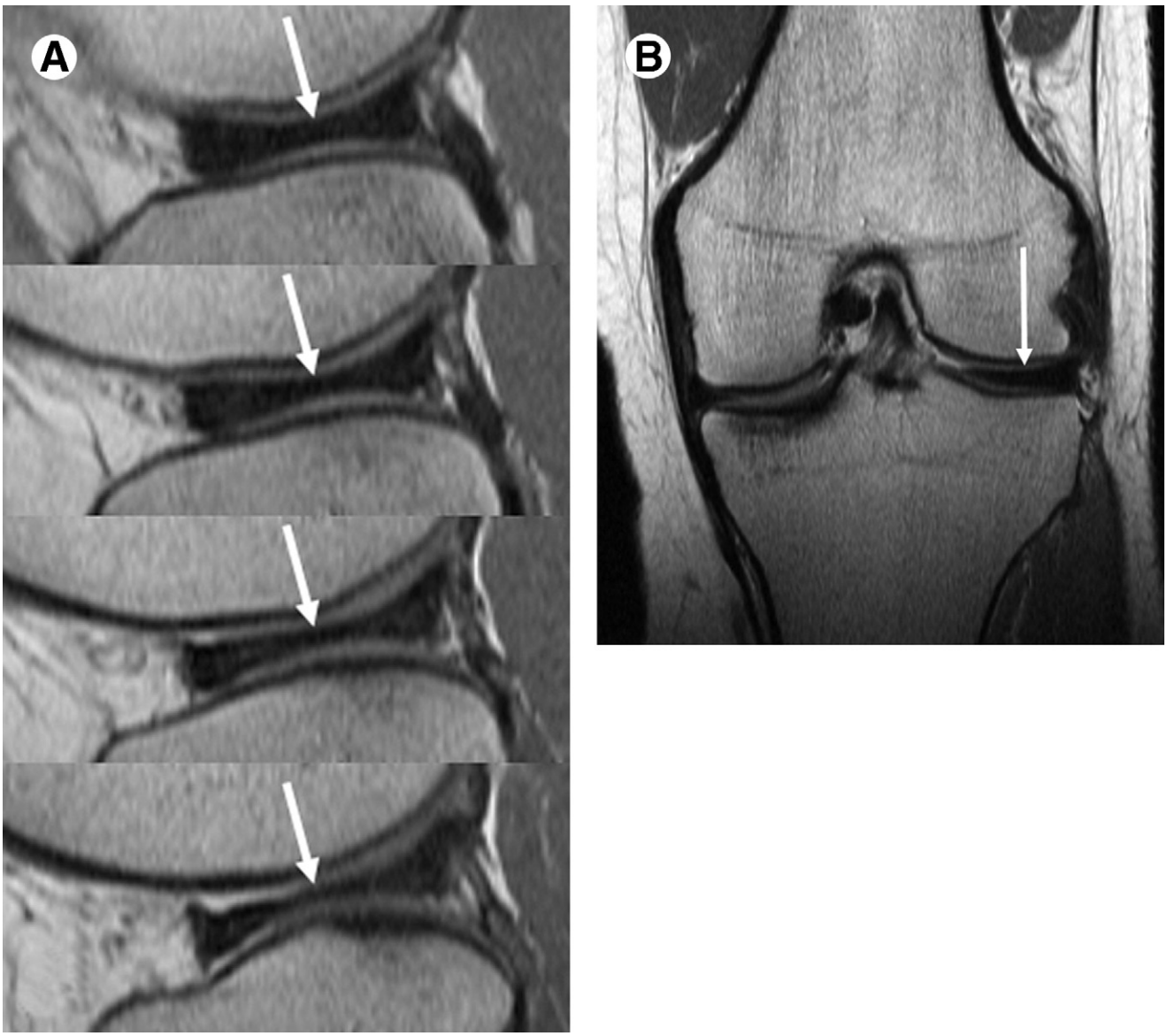

Figure 19 Discoid meniscus. (A) Four consecutive 3-mm sagittal proton density-weighted turbo spin echo images of the central portion of the lateral meniscus show continuity between the anterior and posterior horns (arrows), indicating a discoid meniscus. (B) Coronal proton density-weighted turbo spin echo image through the midportion of the knee demonstrates an abnormally wide lateral meniscal body (arrow), representing a discoid meniscus.

6. Fischer SP, Fox JM, Del Pizzo W, Friedman MJ, Snyder SJ, Ferkel RD: Accuracy of diagnoses from magnetic resonance imaging of the knee. A multi-center analysis of one thousand and fourteen patients. J Bone Joint Surg Am 73(1):2-10, 1991
7. Mackenzie R, Palmer CR, Lomas DJ, Dixon AK: Magnetic resonance imaging of the knee: diagnostic performance studies. Clin Radiol 51(4): 251-257, 1996
8. Maurer EJ, Kaplan PA, Dussault RG, et al: Acutely injured knee: effect of MR imaging on diagnostic and therapeutic decisions. Radiology 204(3):799-805, 1997
9. McNally EG, Nasser KN, Dawson S, Goh LA: Role of magnetic resonance imaging in the clinical management of the acutely locked knee. Skeletal Radiol 31(10):570-573, 2002
10. Nikken JJ, Oei EH, Ginai AZ, et al: Acute peripheral joint injury: cost and effectiveness of low-field-strength MR imaging—results of randomized controlled trial. Radiology 236(3):958-967, 2005
11. Oei EH, Nikken JJ, Ginai AZ, et al: Acute knee trauma: value of a short dedicated extremity MR imaging examination for prediction of subsequent treatment. Radiology 234(1):125-133, 2005
12. American College of Radiology (ACR) and the Society of Skeletal Radiology (SSR). Practice Guideline for the Performance and Interpretation of Magnetic Resonance Imaging (MRI) of the Knee. 2005
13. Cotten A, Delfaut E, Demondion X, et al: MR imaging of the knee at 0.2 and 1.5 T: correlation with surgery. AJR Am J Roentgenol 174(4):1093-1097, 2000
14. Mellado JM, Ramos A, Salvado E, Camins A, Calmet J, Sauri A: Avulsion fractures and chronic avulsion injuries of the knee: role of MR imaging. Eur Radiol 12(10):2463-2473, 2002
15. Kode L, Lieberman JM, Motta AO, Wilber JH, Vasen A, Yagan R: Evaluation of tibial plateau fractures: efficacy of MR imaging compared with CT. AJR Am J Roentgenol 163(1):141-147, 1994
16. Mui LW, Engelsohn E, Umans H: Comparison of CT and MRI in patients with tibial plateau fracture: can CT findings predict ligament tear or meniscal injury? Skeletal Radiol 36(2):145-151, 2007
17. Yu JS, Goodwin D, Salonen D, et al: Complete dislocation of the knee: spectrum of associated soft-tissue injuries depicted by MR imaging. AJR Am J Roentgenol 164(1):135-139, 1995

Figure 20 Meniscal cyst. Coronal T2-weighted turbo spin echo image demonstrates a meniscal cyst of the lateral meniscus (long arrow). The cyst is continuous with a horizontal cleavage tear of the lateral meniscus (short arrow).

18. Virolainen H, Visuri T, Kuusela T: Acute dislocation of the patella: MR findings. Radiology 189(1):243-246, 1993
19. Sanders TG, Medynski MA, Feller JF, Lawhorn KW: Bone contusion patterns of the knee at MR imaging: footprint of the mechanism of injury. Radiographics 20:S135-S151, 2000
20. De Smet AA, Fisher DR, Graf BK, Lange RH: Osteochondritis dissecans of the knee: value of MR imaging in determining lesion stability and the presence of articular cartilage defects. AJR Am J Roentgenol 155(3): 549-553, 1990
21. Robertson PL, Schweitzer ME, Bartolozzi AR, Ugoni A: Anterior cruciate ligament tears: evaluation of multiple signs with MR imaging. Radiology 193(3):829-834, 1994
22. Gentili A, Seeger LL, Yao L, Do HM: Anterior cruciate ligament tear: indirect signs at MR imaging. Radiology 193(3):835-840, 1994
23. Brandser EA, Riley MA, Berbaum KS, el-Khoury GY, Bennett DL: MR imaging of anterior cruciate ligament injury: independent value of primary and secondary signs. AJR Am J Roentgenol 167(1):121-126, 1996
24. Tung GA, Davis LM, Wiggins ME, Fadale PD: Tears of the anterior cruciate ligament: primary and secondary signs at MR imaging. Radiology 188(3):661-667, 1993
25. Umans H, Wimpfheimer O, Haramati N, Applbaum YH, Adler M, Bosco J: Diagnosis of partial tears of the anterior cruciate ligament of the knee: value of MR imaging. AJR Am J Roentgenol 165(4):893-897, 1995
26. Kannus P, Bergfeld J, Jarvinen M, et al: Injuries to the posterior cruciate ligament of the knee. Sports Med 12(2):110-131, 1991
27. Staron RB, Haramati N, Feldman F, et al: O'Donoghue's triad: magnetic resonance imaging evidence. Skeletal Radiol 23(8):633-636, 1994
28. Miller TT, Gladden P, Staron RB, Henry JH, Feldman F: Posterolateral stabilizers of the knee: anatomy and injuries assessed with MR imaging. AJR Am J Roentgenol 169(6):1641-1647, 1997
29. Miller TT, Staron RB, Feldman F, Cepel E: Meniscal position on routine MR imaging of the knee. Skeletal Radiol 26(7):424-427, 1997
30. Crues JV 3rd, Mink J, Levy TL, Lotysch M, Stoller DW: Meniscal tears of the knee: accuracy of MR imaging. Radiology 164(2):445-448, 1987

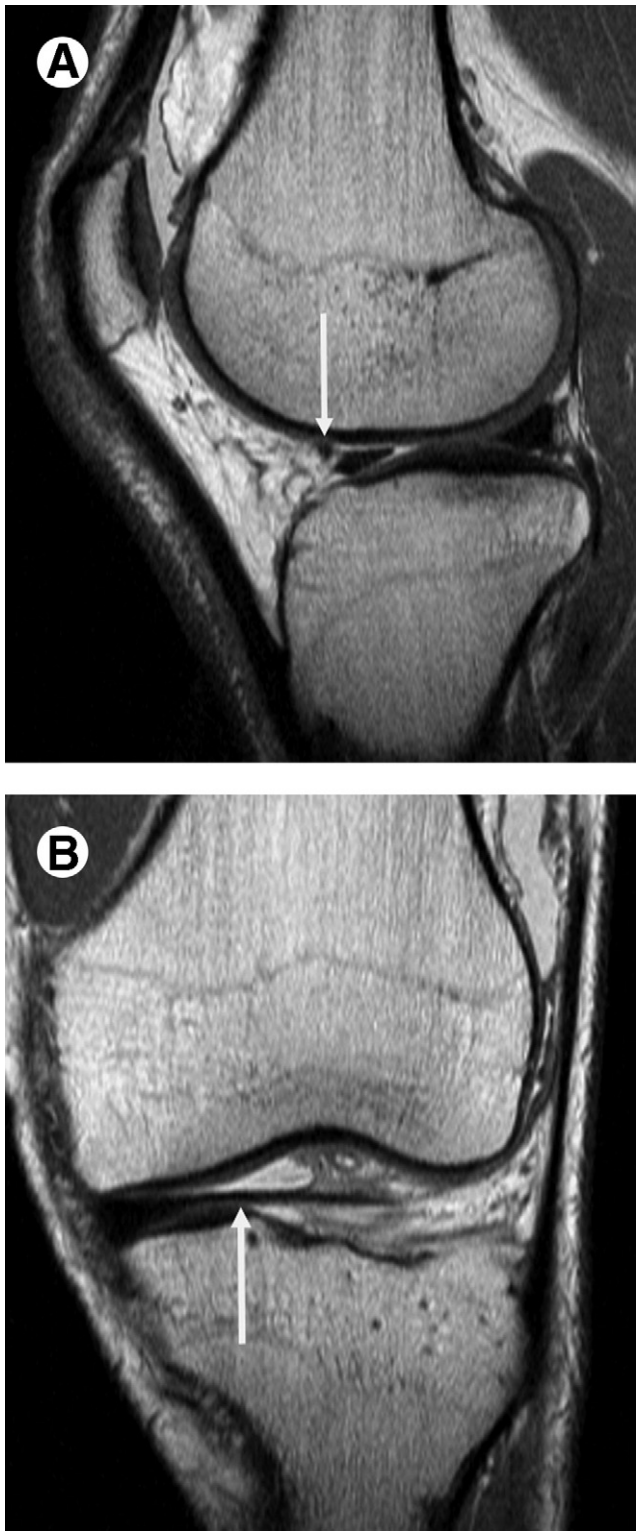

Figure 21 Transverse meniscal ligament. (A) Sagittal proton density-weighted turbo spin echo image. The transverse meniscal ligament (arrow) may mimic a tear of the anterior horn of the lateral meniscus. (B) On the coronal image, the course of the transverse meniscal ligament is nicely shown (arrow).

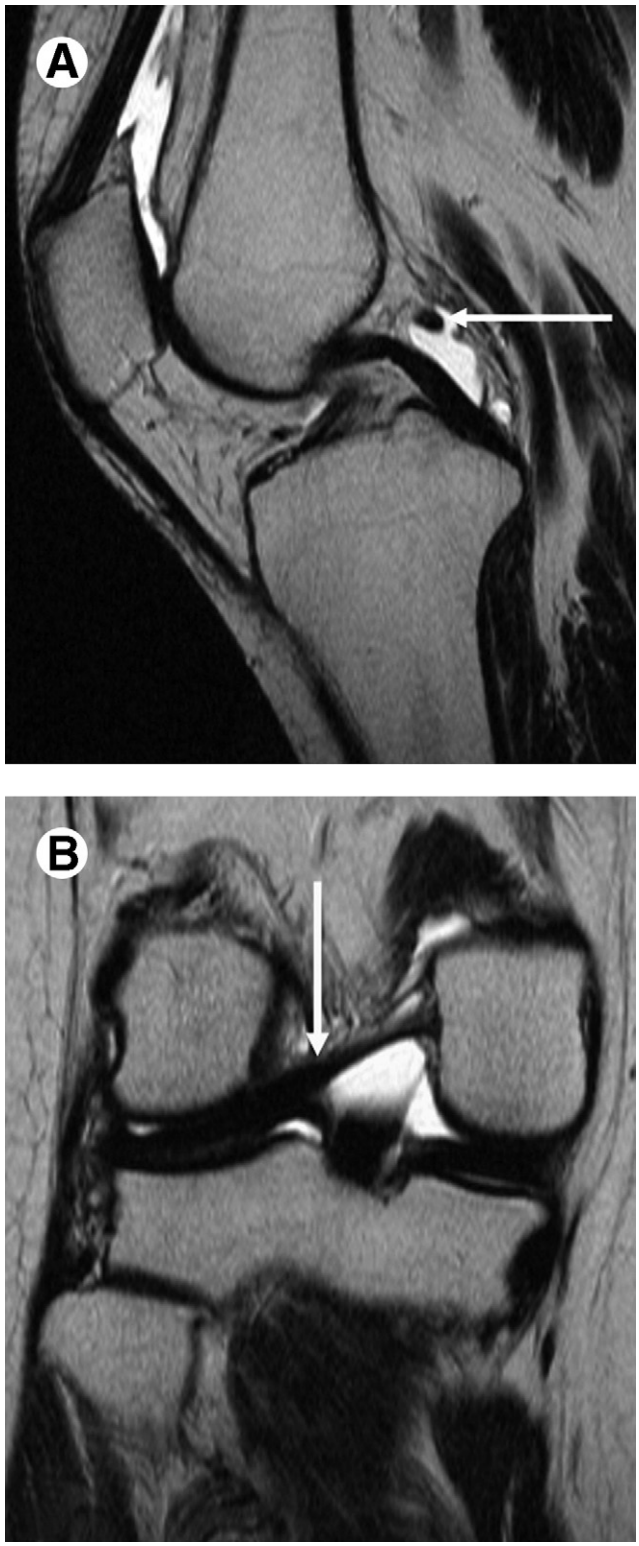

Figure 22 Meniscofemoral ligament of Wrisberg. (A) Sagittal T2-weighted turbo spin echo image. The meniscofemoral ligament of Wrisberg resembles a loose body surrounded by fluid (arrow). (B) The ligament has an unusually thick appearance in this case and is well visualized on the coronal T2-weighted image (arrow).

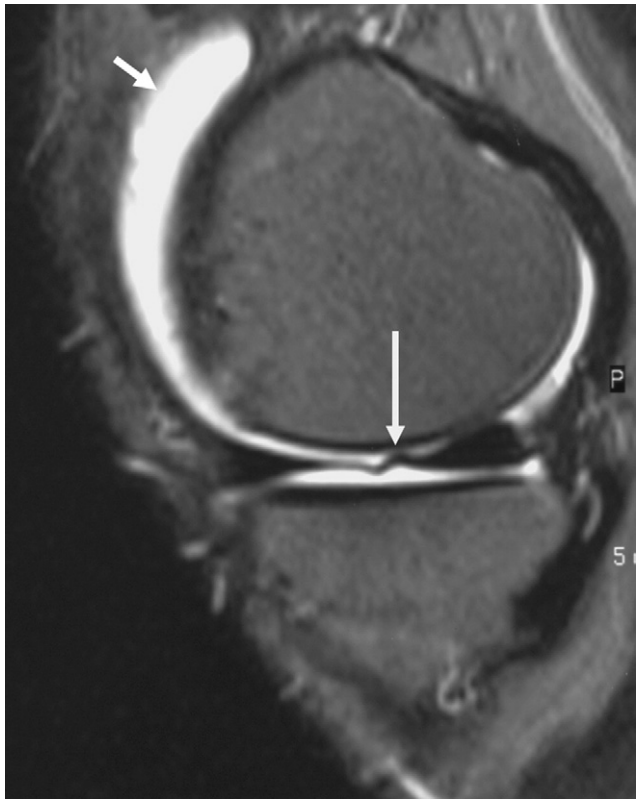

Figure 23 Meniscal flounce. Sagittal T2-weighted turbo spin echo image demonstrates a wrinkled appearance of the central portion of the medial meniscus (arrow), the so-called meniscal flounce. This is a normal variant and should not be misdiagnosed as a tear. In addition, joint effusion is seen in the suprapatellar recess (short arrow).

31. Reicher MA, Hartzman S, Duckwiler GR, Bassett LW, Anderson LJ, Gold RH: Meniscal injuries: detection using MR imaging. Radiology 159(3):753-757, 1986
32. Stoller DW, Martin C, Crues JV 3rd, Kaplan L, Mink JH: Meniscal tears: pathologic correlation with MR imaging. Radiology 163(3):731-735, 1987
33. Boks SS, Vroegindeweij D, Koes BW, Hunink MM, Bierma-Zeinstra SM: Magnetic resonance imaging abnormalities in symptomatic and contralateral knees: prevalence and associations with traumatic history in general practice. Am J Sports Med 34(12):1984-1991, 2006
34. Wright DH, De Smet AA, Norris M: Bucket-handle tears of the medial and lateral menisci of the knee: value of MR imaging in detecting displaced fragments. AJR Am J Roentgenol 165(3):621-625, 1995
35. Dorsay TA, Helms CA: Bucket-handle meniscal tears of the knee: sensitivity and specificity of MRI signs. Skeletal Radiol 32(5):266-272, 2003
36. Magee TH, Hinson GW: MRI of meniscal bucket-handle tears. Skeletal Radiol 27(9):495-499, 1998
37. Singson RD, Feldman F, Staron R, Kiernan H: MR imaging of displaced bucket-handle tear of the medial meniscus. AJR Am J Roentgenol 156(1):121-124, 1991
38. Weiss KL, Morehouse HT, Levy IM: Sagittal MR images of the knee: a low-signal band parallel to the posterior cruciate ligament caused by a displaced bucket-handle tear. AJR Am J Roentgenol 156(1):117-119, 1991
39. Helms CA, Laorr A, Cannon WD Jr: The absent bow tie sign in bucket-handle tears of the menisci in the knee. AJR Am J Roentgenol 170(1): 57-61, 1998
40. Watt AJ, Halliday T, Raby N: The value of the absent bow tie sign in MRI of bucket-handle tears. Clin Radiol 55(8):622-626, 2000

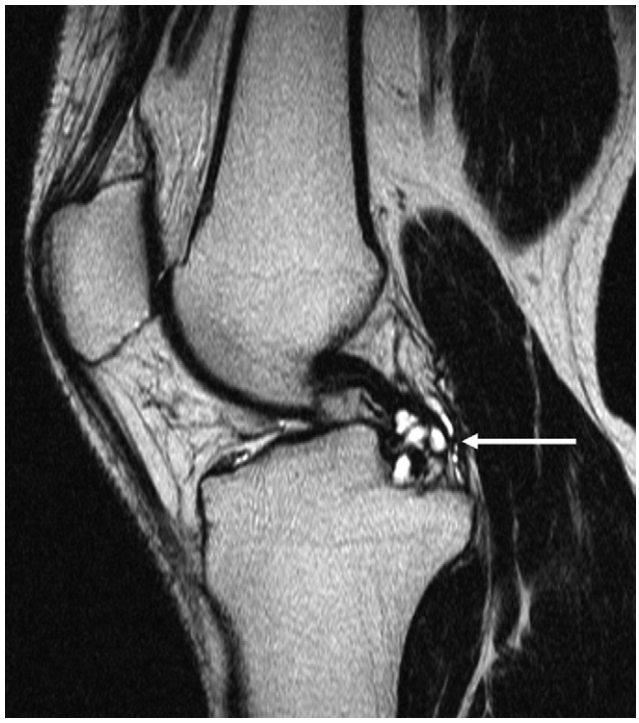

Figure 24 PCL ganglion. Sagittal T2-weighted turbo spin echo image. A well-defined globular lesion with high signal intensity is seen surrounding the distal portion of the PCL (arrow), representing a ganglion of the PCL.

41. Haramati N, Staron RB, Rubin S, Shreck EH, Feldman F, Kiernan H: The flipped meniscus sign. Skeletal Radiol 22(4):273-277, 1993
42. Silverman JM, Mink JH, Deutsch AL: Discoid menisci of the knee: MR imaging appearance. Radiology 173(2):351-354, 1989
43. Samoto N, Kozuma M, Tokuhisa T, Kobayashi K: Diagnosis of discoid lateral meniscus of the knee on MR imaging. Magn Reson Imaging 20(1):59-64, 2002
44. Campbell SE, Sanders TG, Morrison WB: MR imaging of meniscal cysts: incidence, location, and clinical significance. AJR Am J Roentgenol 177(2):409-413, 2001
45. Tyson LL, Daughters TC Jr, Ryu RK, Crues JV 3rd: MRI appearance of meniscal cysts. Skeletal Radiol 24(6):421-424, 1995
46. Park JS, Ryu KN, Yoon KH: Meniscal flounce on knee MRI: correlation with meniscal locations after positional changes. AJR Am J Roentgenol 187(2):364-370, 2006
47. Yu JS, Cosgarea AJ, Kaeding CC, Wilson D: Meniscal flounce MR imaging. Radiology 203(2):513-515, 1997
48. Kim BH, Seol HY, Jung HS, Cha SH, Park CM, Lim HC: Meniscal flounce on MR: correlation with arthroscopic or surgical findings. Yonsei Med J 41(4):507-511, 2000
49. Recht MP, Applegate G, Kaplan P, et al: The MR appearance of cruciate ganglion cysts: a report of 16 cases. Skeletal Radiol 23(8):597-600, 1994
50. Craig JG, Go L, Blechinger J, et al: Three-tesla imaging of the knee: initial experience. Skeletal Radiol 34(8):453-461, 2005
51. Magee T, Williams D: 3.0-T MRI of meniscal tears. AJR Am J Roentgenol 187(2):371-375, 2006
52. Ramnath RR, Magee T, Wasudev N, Murrah R: Accuracy of 3-T MRI using fast spin-echo technique to detect meniscal tears of the knee. AJR Am J Roentgenol 187(1):221-225, 2006
53. Lutterbey G, Behrends K, Falkenhausen MV, et al: Is the body-coil at 3 Tesla feasible for the MRI evaluation of the painful knee? A comparative study Eur Radiol 17:503-508, 2007
54. Tins BJ, McCall IW, Takahashi T, et al: Autologous chondrocyte implantation in knee joint: MR imaging and histologic features at 1-year follow-up. Radiology 234(2):501-508, 2005
55. James SL, Connell DA, Saifuddin A, Skinner JA, Briggs TW: MR imaging of autologous chondrocyte implantation of the knee. Eur Radiol 16(5):1022-1030, 2006
56. Yoshioka H, Alley M, Steines D, et al: Imaging of the articular cartilage in osteoarthritis of the knee joint: 3D spatial-spectral spoiled gradient-echo vs. fat-suppressed 3D spoiled gradient-echo MR imaging. J Magn Reson Imaging 18(1):66-71, 2003
57. Reeder SB, Pelc NJ, Alley MT, Gold GE: Rapid MR imaging of articular cartilage with steady-state free precession and multipoint fat-water separation. AJR Am J Roentgenol 180(2):357-362, 2003
58. Kornaat PR, Reeder SB, Koo S, et al: MR imaging of articular cartilage at 1.5T and 3.0T: comparison of SPGR and SSFP sequences. Osteoarthritis Cartilage 13(4):338-344, 2005
59. Gold GE, Reeder SB, Yu H, et al: Articular cartilage of the knee: rapid three-dimensional MR imaging at 3.0 T with IDEAL balanced steady-state free precession–initial experience. Radiology 240(2):546-551, 2006
60. Kornaat PR, Koo S, Andriacchi TP, Bloem JL, Gold GE: Comparison of quantitative cartilage measurements acquired on two 3.0T MRI systems from different manufacturers. J Magn Reson Imaging 23(5):770-773, 2006